

A Bio-Resonant Blueprint:

A Methodology for Calculating the Electrical Frequencies of Human Cells and Their Resonant Irradiation with Geo Equipment.

Research and documentation by Artur Lanz
RadiantPhi

Introduction by the Principal Investigator

The following document, along with the accompanying comprehensive list, represents the culmination of an independent research endeavor I initiated in 2018. My background is in engineering, and my focus has consistently been on uncovering the fundamental principles that govern complex systems. I quickly recognized that the most intricate and elegant system we understand, the human body, was predominantly examined through the lens of biochemistry, while its essential electrical properties remained largely uninvestigated in clinical practice.

My hypothesis was straightforward: if life is a bioelectric phenomenon, then each cell must function with a distinct electrical signature. This paper outlines the methodology I devised to map these signatures and the technology developed to engage with them—a connection between the principles of field physics and biological function.

1. The Fundamental Principle: The Cell as a Resonant Circuitry

From an engineering standpoint, a biological cell represents a resonant circuit of remarkable elegance. Its lipid bilayer membrane acts as a capacitor (insulator), delineating two conductive environments: the cytoplasm and the extracellular fluid. This system inherently exhibits a characteristic frequency at which its response to an external electric field is optimized.

This phenomenon, referred to in biophysics as beta scattering (β -scattering), arises from membrane polarization induced by a high-frequency field (Maxwell-Wagner effect). It is not a mechanical resonance; instead, it represents the optimal efficiency of electrical charging and discharging of the cell membrane. This is the resonance signature we have modeled.

I2. Methodology: The Predictive Model of Cellular Resonance

To translate this principle into a predictive map, a validated biophysical model, referred to as the single-shell spherical model, was employed.

The Mathematical Model: Each cell is conceptualized as a perfect sphere, a simplification that enables the application of a robust formula derived from bioimpedance theory to determine its characteristic frequency.

The Central Formula: The frequency (f_c) is determined using the following fundamental equation:

$$f_c = 1 / (2 * \pi * r * C_m * (1/\sigma_i + 1/\sigma_e))$$

Constants and Parameters Utilized:

Cellular Radius (r): The primary variable derived from histological literature that distinguishes each cell type.

Membrane Capacitance (C_m): A standard value of 0.01 Farads/m² (1 μ F/cm²) was employed, reflecting the capacitance of the lipid bilayer approximately 8 nm in thickness.

Cytoplasmic Conductivity (σ_i): A value of 0.8 Siemens per meter (S/m) was assumed to model the intracellular ionic environment.

Extracellular Conductivity (σ_e): A value of 0.8 S/m was assumed, reflecting an isotonic tissue environment.

The Model's Key Discovery: The formula uncovers a sophisticated, inversely proportional relationship: larger cells resonate at lower frequencies, whereas smaller cells resonate at higher frequencies.

3. Applied Technology: RadiantPhi High-Frequency Field Devices.

Since 2018, I have engineered devices that generate biocompatible fields grounded in these principles. The apparatus employed is a high-frequency (HF) field emitter, characterized by three essential operating features:

High Voltage: To create a well-defined and impactful potential field.

Negative Polarity Charge: To assist in restoring the natural electrical potential of cellular membranes.

Limited Nonlinear Emissions: The technology does not produce a straightforward sine wave. Rather, it creates a complex, harmonic-rich field focused on the target resonant frequency. This facilitates the efficient transmission of biophysical information without imparting detrimental thermal energy.

4. Insights and Aspirations for the Future.

The utilization of the specific frequencies outlined in the subsequent list, via this technology, has been the focal point of my empirical research. Although thorough clinical validation is necessary, we have consistently noted a diverse array of beneficial physiological responses in biological systems, indicating a propensity for self-regulation and homeostasis.

The patient presented with an external hordeolum ("stye") characterized by edema, erythema, and swelling, prompting her physician to recommend surgical drainage. Two sessions of Geo/Plasma therapy were conducted on consecutive days utilizing high-frequency electrodes, applied for 25 minutes, beginning around the affected area and gradually moving closer until gently passing over the lesion. No alternative methods or additional treatments were employed. The initial photograph depicts acute inflammation; the second, taken the day following the first session, illustrates a marked reduction in edema and erythema; and the third, captured after the second session, demonstrates nearly complete resolution of the inflammatory process without the necessity for invasive intervention, accompanied by progressive normalization of the periocular tissue.

This list is not intended as an unchanging law but rather as a foundational blueprint: an initial comprehensive map of the human body's resonance spectrum. It serves as a catalyst for a new era of research in bioelectrical medicine, enabling us to communicate with our cells in the language they comprehend most effectively: the language of frequency.



5. Model Validation: Transitioning from Theory to Spectral Evidence

A mathematical model, regardless of its robustness, must be anchored in empirical reality. Prior to unveiling the comprehensive framework of cellular frequencies, it is essential to establish that the principles of harmonic resonance and coherent emission, which underpin our work, are not merely theoretical constructs but rather measurable and repeatable characteristics of our technology.

The following section provides the spectral analysis of RadiantPhi's GEO/PLASMA and GEO/COMPACT devices. These measurements are not intended to identify the resonance of a specific cell; instead, they aim to validate the capacity of our GEO generators to produce coherent and structured electromagnetic fields essential for interaction with biological systems at the cellular level.

5.1 Certification of the Device Under Test and Measurement Methodology

Every measurement is only as reliable as the instrument conducting it and the object being measured. To ensure maximum transparency, we have included the Certificate of Authenticity for the device under evaluation: the GEO Generator, meticulously designed and calibrated by engineer Artur Lanz. This certificate guarantees that the GEO equipment, whose emissions we are measuring, comprises original systems constructed to ensure electromagnetic coherence, harmonic purity, and negative charge stability.

Spectral measurements were conducted under controlled laboratory conditions in Puerto Morelos, Quintana Roo. Data acquisition utilized a Rigol DSA815-TG spectrum analyzer, safeguarded by a Faraday cage, in conjunction with a high-impedance RF probe. This configuration facilitated the accurate capture of the emission signature from the GEO generators, reducing interference and ensuring data integrity.

5.2 Spectroscopic Analysis of GEO Systems

The graphs presented in the appendices of this document illustrate the emission signature of the GEO systems, as captured by the Rigol analyzer. Upon examination, we identified several critical points that corroborate our methodology:

Coherent and Harmonic Emission: The recorded spectrum is not mere random noise; rather, it represents a non-linear emission characterized by coherent harmonics, systematically organized along the observed band.

Resonant and Multipoint Nature: Measurements of the various "taps" or output configurations of the GEO/COMPACT generator reveal a consistent spectral signature, albeit with variations in amplitude and harmonic density. This illustrates the GEO system's characteristics as a multipoint resonator, adept at preserving the overall coherence of the pattern while adjusting its energy equilibrium point.

Longitudinal Field and Electric Potential: The harmonic structure and estimated effective voltage (6,000 to 10,000 volts RMS) are indicative of a longitudinal field exhibiting a negative charge. The energy emitted by the GEO system is not conveyed as a conventional current but rather as an organized potential gradient. This distinction is vital, as it is this specific type of potential field that can directly interact with the cell membrane, polarizing it without imparting detrimental thermal energy.

5.3 Validation Summary

The spectral measurements provided are unequivocal: RadiantPhi's GEO generator technology can generate coherent electromagnetic fields, abundant in harmonics and resonant in nature, precisely the type of emission required to interact effectively with the frequency signatures of biological systems.

This empirical evidence instills confidence in asserting that the interactions observed in biological systems are neither a placebo effect nor mere coincidence. Rather, they result from a genuine dialogue between a structured information field, produced by our equipment, and the cell's intrinsic resonance.

6. The Conclusive Theoretical Framework: The Bioelectrodynamics of the Resonant Body

The frequency list included in the appendices transcends a mere numerical exercise; it serves as a representation of a vibrant, dynamic, and fundamentally electrical domain. To grasp its full significance, we must delineate the biophysical framework that supports it: a body that is not simply an assemblage of chemicals, but rather a cohesive electromagnetic network, wherein signals traverse a crystalline conductive medium.

6.1 Bioelectricity: Physiological Facts, Not Speculation

Skepticism regarding the body's "electricity" is prevalent, frequently stemming from semantic misunderstandings. Bioelectricity does not refer to the flow of electrons in a copper wire; rather, it pertains to ionic electrostatics, which underpins neurophysiology.

The Physical Definition is Realized: Electric current is, by definition, the movement of charge. In our nerves, the moving charges consist of ions (Na^+ , K^+ , Ca^{2+} , Cl^-). This flow produces measurable potential differences (approximately -70 mV at rest) and currents (in picoamperes and nanoamperes). This is not merely an analogy; it is electricity.

The Action Potential: The Electrical Pulse of Life: A nerve impulse represents a self-propagating wave of electrical depolarization. A stimulus activates sodium (Na^+) channels, briefly reversing the membrane potential and producing an electrical pulse that propagates along the axon. The subsequent efflux of potassium (K^+) repolarizes the membrane, priming it for the next pulse. This phenomenon is digital, quantifiable, and predictable.

The Axon as a Biological Waveguide: From a physics standpoint, the axon can be effectively modeled through Cable Theory. This theory elucidates the propagation of voltage along a resistive-capacitive framework. The membrane functions as the capacitor (C_m), while the cytoplasm and extracellular fluid serve as the resistors (r_i , r_e). The propagation of voltage (V) over time (t) and space (x) is characterized by:

$\lambda^2 * (\partial^2 V / \partial x^2) = \tau * (\partial V / \partial t) + V$, where λ (lambda) represents the spatial constant and τ (tau) denotes the temporal constant of the membrane. The action potential is, in essence, the solution to this equation manifested as a traveling wave.

Irrefutable Evidence: This is not a matter of opinion but rather of direct measurement. EEG, EMG, and ECG monitor the electrical activity of the brain, muscles, and heart. The Patch-Clamp technique records individual ionic currents. Therapies such as pacemakers and deep brain stimulation modulate circuits precisely because they respond to fields and currents. The dichotomy of "chemistry vs. electricity" is misleading. It is an electrochemical system: chemical gradients serve as the energy source, while ionic electrical currents facilitate the conversion of that energy into information.

6.2 The Conductive Medium: The Crystalline Water Matrix

Having established the reality of electrical signals, the subsequent inquiry is: how do they propagate with such coherence within a biological medium? The response lies in the fact that current favors order, and bodily fluids are not amorphous liquids.

The Physics of Conduction: Order is Efficiency: In a crystal, an organized atomic lattice provides a low-resistance pathway for charge flow. In a disordered medium, energy dissipates, resulting in a loss of signal coherence. The human body has addressed this challenge by utilizing water in a remarkable manner.

The Fourth State of Water: A Biological Liquid Crystal: As illustrated by pioneers such as Gerald Pollack and Esther del Río, water interacting with hydrophilic surfaces (membranes, proteins) spontaneously arranges itself into a highly structured phase, akin to a liquid crystal. This "Exclusion Zone Water" (EZ Water) exhibits remarkable properties:

Hexagonal Structure: H₂O molecules arrange themselves in a systematic and stable network.

Charge Separation: Establishes a region with a net negative charge, generating a spontaneous electrical potential, akin to a biological battery energized by the infrared light present in the environment.

Proton Conductivity: It functions as a natural semiconductor, enabling the movement of protons (H⁺) and other charges with remarkably low resistance.

The Intelligent Matrix: This structured water network is not merely a solvent; it serves as an active and essential element of the body's circuitry. It functions as a network that directs, safeguards, and synchronizes bioelectrical signals. In a healthy and adequately hydrated condition, this crystalline matrix remains coherent. However, during dehydration or oxidative stress, the matrix loses its structure, resulting in increased impedance and diminished signal fidelity.

6.3 Final Synthesis: The Body as a Bio-Resonant Network

When we integrate these two concepts, a comprehensive and profoundly optimistic perspective of biology unfolds. We are not merely "chemical machines," but rather living circuits through which coherent electrical signals traverse an intelligent liquid crystal array.

The signals consist of action potentials and various ionic flows, representing the digital language of our nervous and cellular systems.

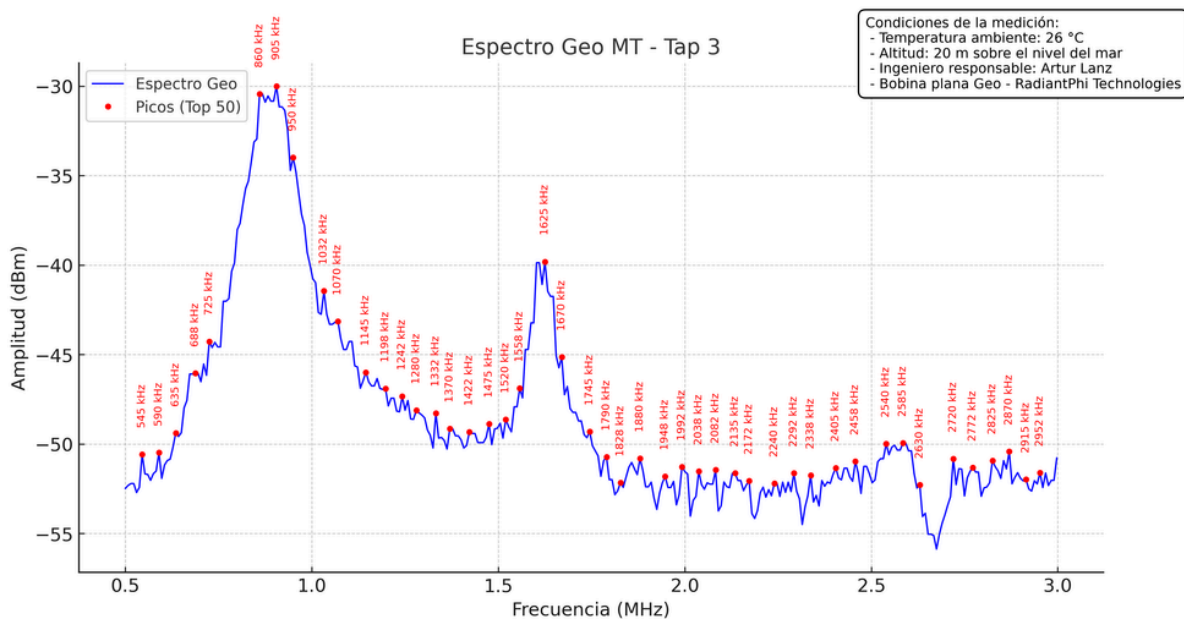
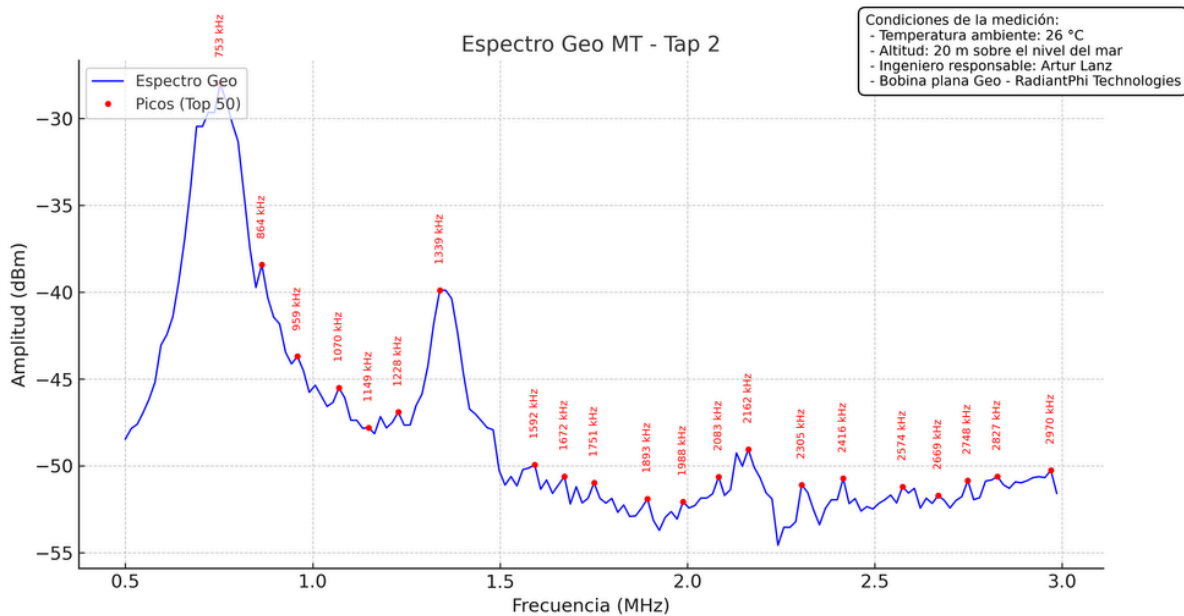
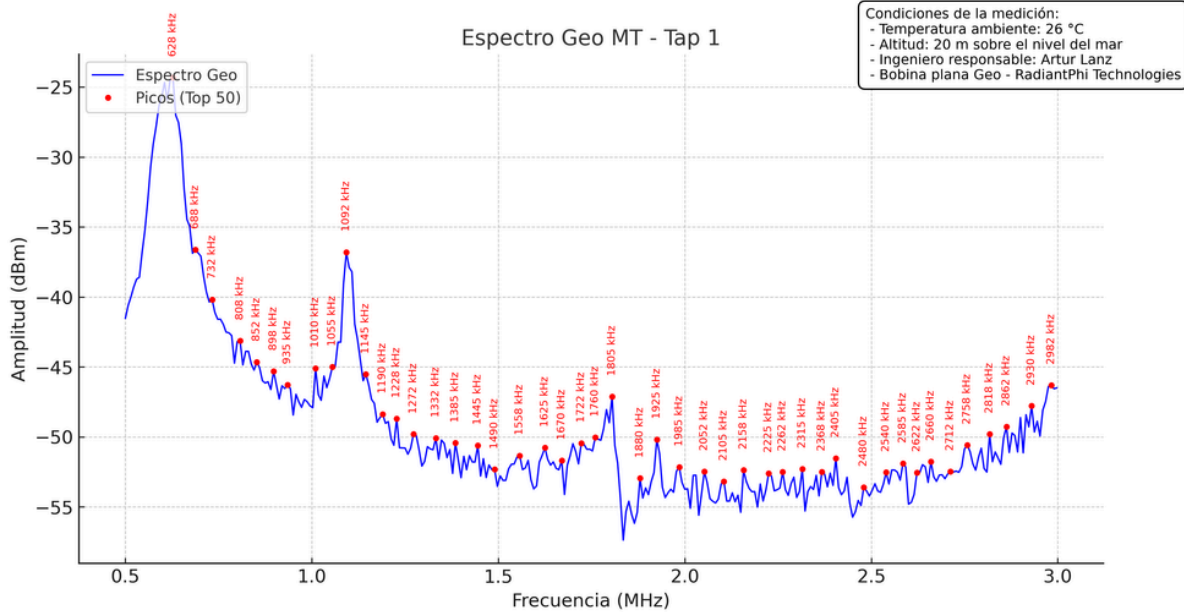
The medium is the organized water network, the cabling that guarantees the message is transmitted clearly and coherently.

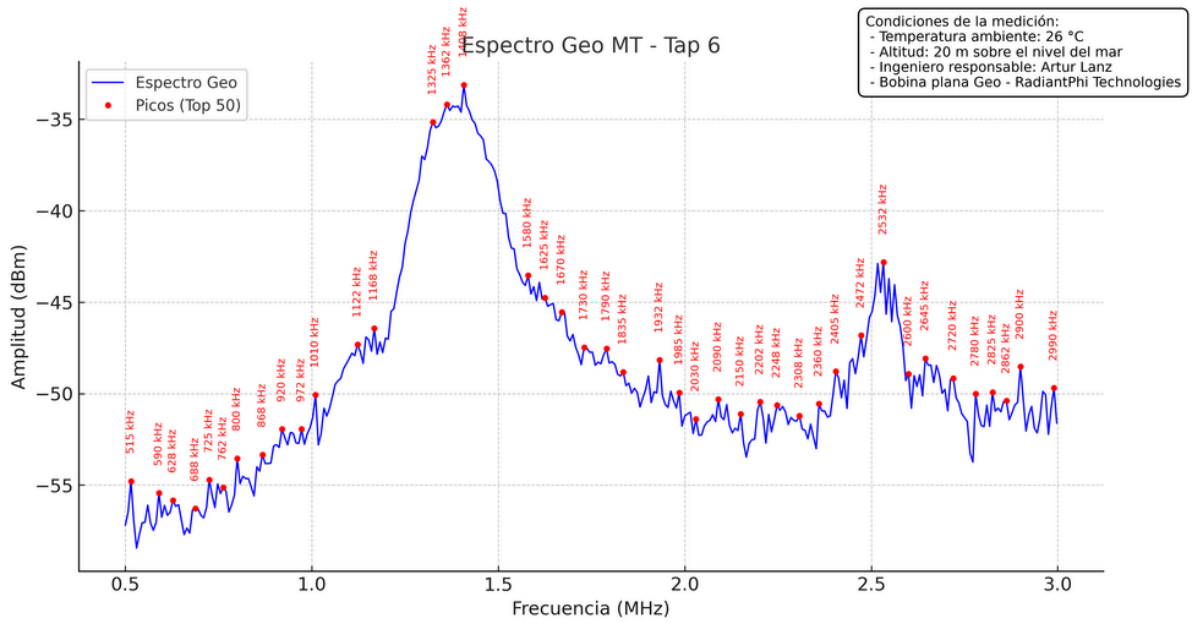
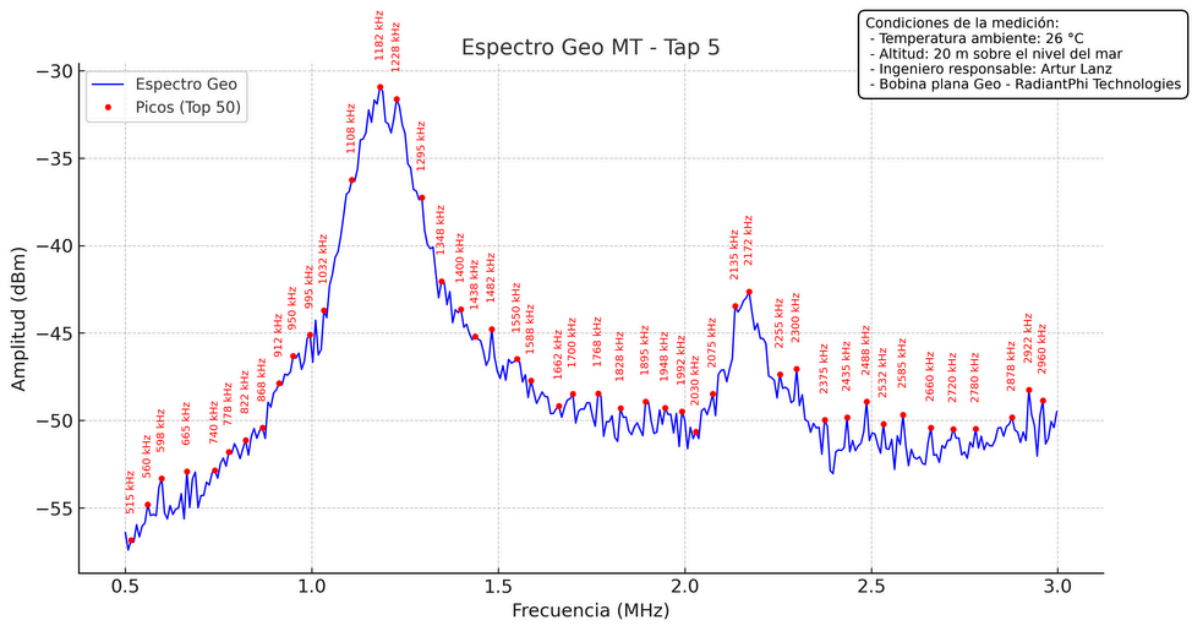
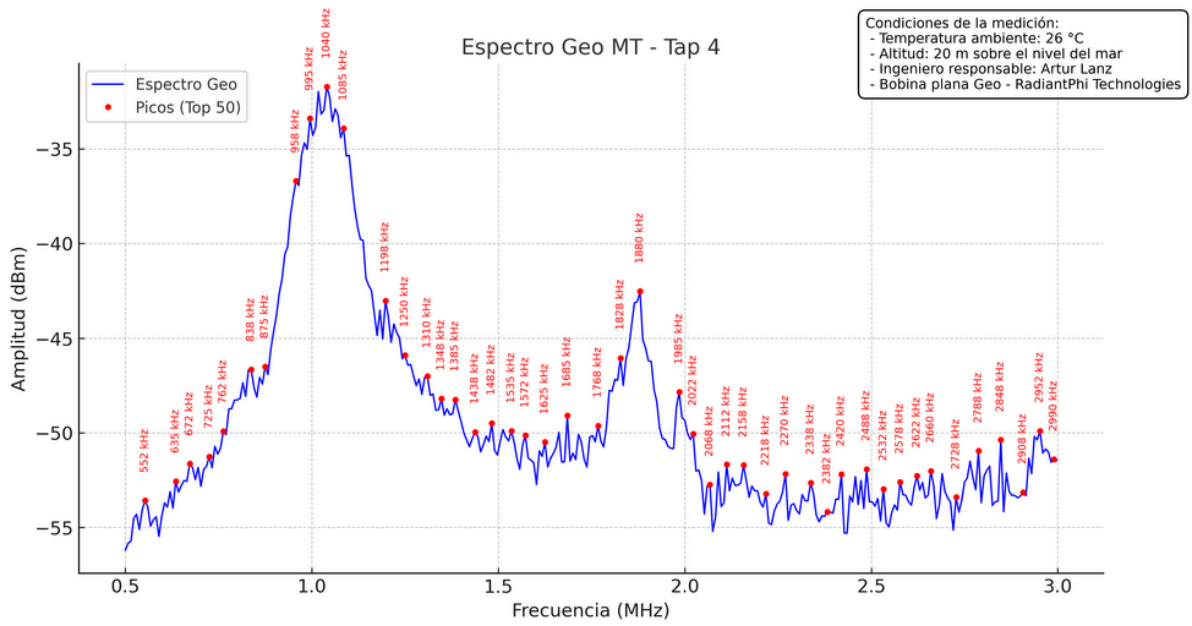
From this perspective, health encompasses not merely chemical balance but also electromagnetic coherence. It involves the integrity of the signal and the quality of the conductive medium. Conversely, disease may be perceived as a "loss of signal" or "noise in the system," resulting from the disruption of this conductive matrix.

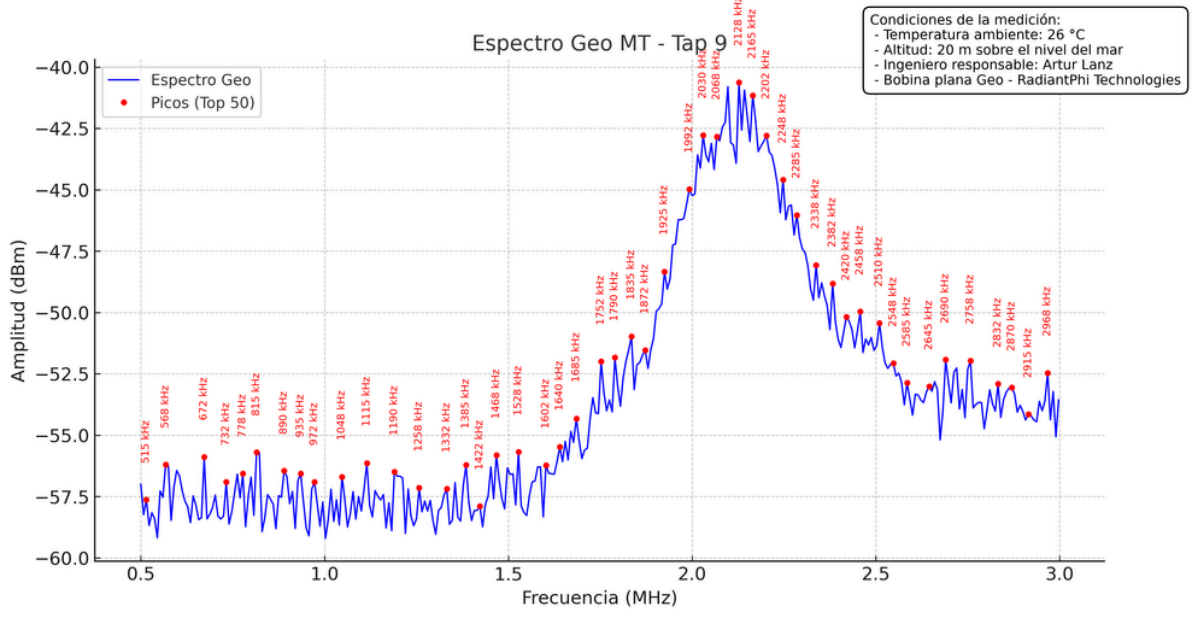
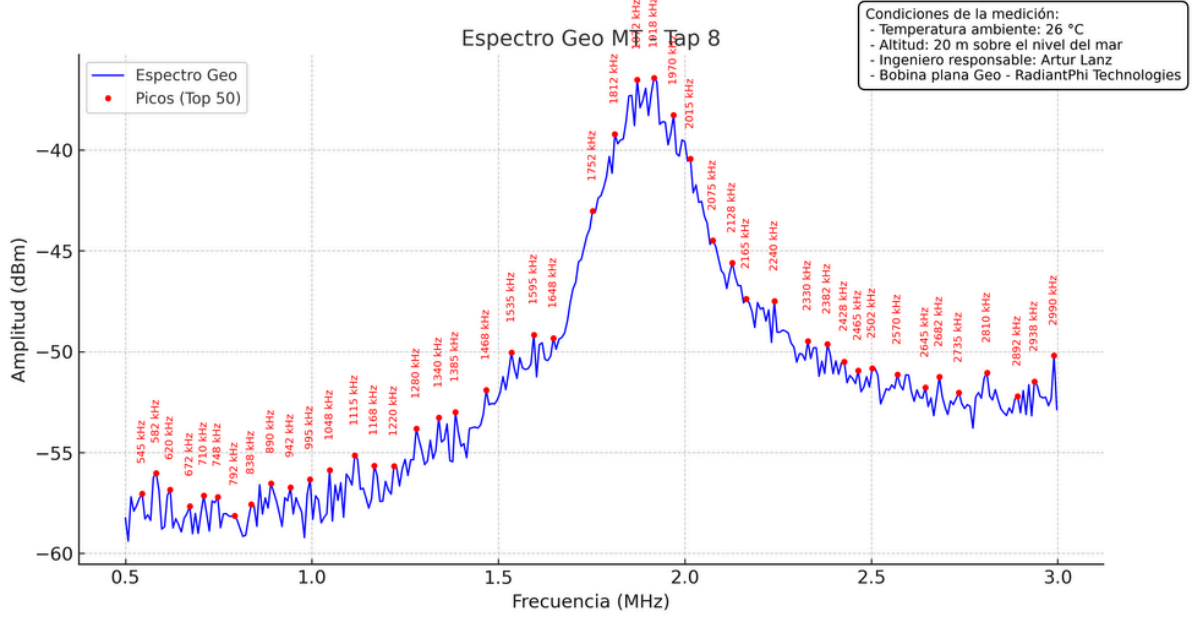
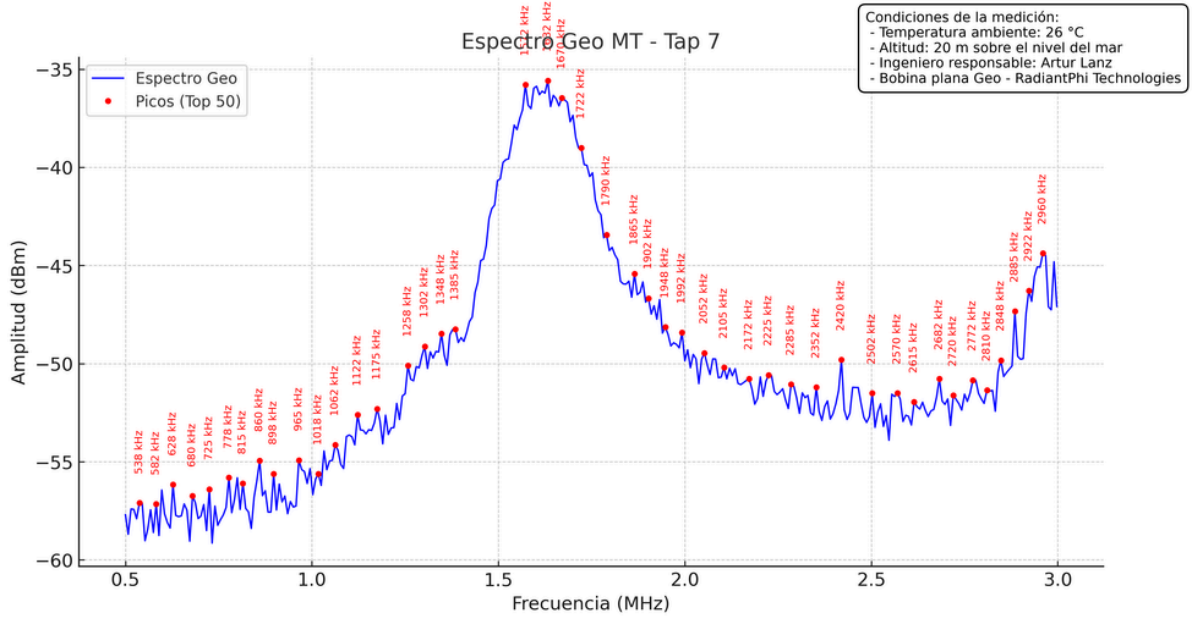
RadiantPhi's approach is grounded in this understanding. We do not aim to impose force upon the body through sheer energy; instead, we strive to communicate with it in its intrinsic language. Our objective is to restore coherence to the conductive matrix and reintroduce the essential "notes" of cellular resonance, thereby reminding the system of its optimal state of harmony.

We are fundamentally a bioelectric symphony. For the first time, we are now learning to interpret the score.

Geo/Compact Spectroscopy







Comprehensive List of 200 Cells and Their Theoretical Resonance Frequencies

The following is a compilation of 200 varieties of human cells along with their determined characteristic resonance frequencies.

BLOOD CELLS AND THE IMMUNE SYSTEM

1	Erythrocyte (Red Blood Cell)	Blood	7.5 μm	8 nm	1.68 MHz
2	Platelet (Thrombocyte)	Blood	3 μm	8 nm	4.20 MHz
3	Reticulocito	Blood (Erythrocyte Precursor)	9 μm	8 nm	1.40 MHz
4	Megacariocito	Bone Marrow	70 μm	8 nm	180 kHz
5	Neutrophil	Immune	12 μm	8 nm	1.05 MHz
6	Eosinophil	Immune	13 μm	8 nm	0.97 MHz
7	Basophil	Immune	15 μm	8 nm	0.84 MHz
8	Monocyte	Immune	18 μm	8 nm	0.70 MHz
9	Macrophage	Immune	21 μm	8 nm	0.60 MHz
10	Osteoclast	Immune System / Skeletal System	100 μm	8 nm	126 kHz
11	Microglia	Immune (CNS)	10 μm	8 nm	1.26 MHz
12	Kupffer cell	Hepatic Immunity	18 μm	8 nm	0.70 MHz
13	Alveolar Macrophage	Pulmonary Immunity	20 μm	8 nm	0.63 MHz
14	Langerhans cell	Pulmonary Immunity	12 μm	8 nm	1.05 MHz
15	Mastocyte	Pulmonary Immunity	20 μm	8 nm	0.63 MHz
16	Dendritic Cell	Pulmonary Immunity	15 μm	8 nm	0.84 MHz
17	Lymphocyte	Pulmonary Immunity	8 μm	8 nm	1.58 MHz
18	B lymphocyte	Pulmonary Immunity	8 μm	8 nm	1.58 MHz
19	Plasma Cell	Pulmonary Immunity	14 μm	8 nm	0.90 MHz
20	Memory Cell B	Pulmonary Immunity	8 μm	8 nm	1.58 MHz
21	T lymphocyte	Pulmonary Immunity	7 μm	8 nm	1.80 MHz
22	Helper T lymphocyte	Pulmonary Immunity	7 μm	8 nm	1.80 MHz
23	Cytotoxic T cell	Pulmonary Immunity	7 μm	8 nm	1.80 MHz
24	Regulatory T Cell	Pulmonary Immunity	7 μm	8 nm	1.80 MHz
25	Natural Killer (NK) Cell	Pulmonary Immunity	12 μm	8 nm	1.05 MHz

CELLS OF THE NERVOUS SYSTEM

26	Neuron (small soma)	Tense	10 μm	8 nm	1.26 MHz
27	Cerebellar Granule Cell	Central Nervous System (CNS)	6 μm	8 nm	2.10 MHz
28	Pyramidal neuron (soma)	Central Nervous System (CNS)	20 μm	8 nm	0.63 MHz
29	Purkinje cell (soma)	Central Nervous System (CNS)	35 μm	8 nm	360 kHz
30	Motor neuron (cell body)	Central Nervous System (CNS)	50 μm	8 nm	252 kHz
31	Interneuron (soma)	Central Nervous System (CNS)	15 μm	8 nm	0.84 MHz
32	Martinotti cell	Central Nervous System (CNS)	18 μm	8 nm	0.70 MHz
33	Astrocito	Glial cells (SNC)	15 μm	8 nm	0.84 MHz
34	Oligodendrocyte	Glial cells (SNC)	12 μm	8 nm	1.05 MHz
35	Schwann cell	Glial Cells (SNP)	25 μm	8 nm	0.50 MHz
36	Ependymal Cell	Glial cells (SNC)	15 μm	8 nm	0.84 MHz
37	Tanicito	Glial cells (SNC)	10 μm	8 nm	1.26 MHz
38	Satellite Glial Cell	Glial Cells (SNP)	8 μm	8 nm	1.58 MHz
39	Photoreceptor (Rod)	Rain (Retina)	2 μm	8 nm	6.30 MHz
40	Photoreceptor (Cone)	Rain (Retina)	5 μm	8 nm	2.52 MHz
41	Bipolar Cell of the Retina	Rain (Retina)	10 μm	8 nm	1.26 MHz
42	Retinal Ganglion Neuron	Rain (Retina)	20 μm	8 nm	0.63 MHz
43	Amacrine cell	Rain (Retina)	8 μm	8 nm	1.58 MHz
44	Lateral Cell	Rain (Retina)	12 μm	8 nm	1.05 MHz
45	Inner Ciliated Cell	Inner Ear	10 μm	8 nm	1.26 MHz
46	External Ciliated Cell	Inner Ear	9 μm	8 nm	1.40 MHz
47	Olfactory Neuron	Olfactory epithelium	5 μm	8 nm	2.52 MHz
48	Flavor Cell	Taste receptor	10 μm	8 nm	1.26 MHz
49	Merkel cell	Dermis (Tactile)	15 μm	8 nm	0.84 MHz

MUSCLE AND SKELETAL CELLS

50	Skeletal Myocyte	Muscle	50 μm	8 nm	252 kHz
51	Cardiomyocito	Heart	25 μm	8 nm	0.50 MHz
52	Smooth Muscle Cell	Muscle	8 μm	8 nm	1.58 MHz
53	Satellite Cell (Muscle)	Muscle	7 μm	8 nm	1.80 MHz
54	Myofibroblasto	Connective Tissue	15 μm	8 nm	0.84 MHz
55	Fibroblasto	Connective Tissue	20 μm	8 nm	0.63 MHz
56	White Adipocyte	Adipose Tissue	90 μm	8 nm	140 kHz
57	Brown Adipocyte	Adipose Tissue	30 μm	8 nm	420 kHz
58	Chondrocyte	Cartilage	15 μm	8 nm	0.84 MHz
59	Osteoblasto	Bone	20 μm	8 nm	0.63 MHz
60	Osteocito	Bone	15 μm	8 nm	0.84 MHz
61	Bone Lining Cell	Bone	10 μm	8 nm	1.26 MHz
62	Tenocito	Tendon	15 μm	8 nm	0.84 MHz

EPITHELIAL AND INTEGUMENTARY CELLS (DERMIS)

63	Keratinocyte (Basal Layer)	Fur	12 μm	8 nm	1.05 MHz
64	Keratinocyte (Stratum Spinosum)	Fur	15 μm	8 nm	0.84 MHz
65	Melanocito	Fur	10 μm	8 nm	1.26 MHz
66	Hair Follicle Cell	Fur	10 μm	8 nm	1.26 MHz
67	Sebocyte (Sebaceous Gland)	Fur	20 μm	8 nm	0.63 MHz
68	Sweat Gland Cell	Fur	15 μm	8 nm	0.84 MHz
69	Simple Squamous Epithelium	Coating	25 μm	8 nm	0.50 MHz
70	Endothelium	Vascular Structures	15 μm	8 nm	0.84 MHz
71	Mesotelio	Body Cavities	20 μm	8 nm	0.63 MHz
72	Simple Cuboidal Epithelium	Tubules / Ducts	15 μm	8 nm	0.84 MHz
73	Simple Columnar Epithelium	Digestive / Respiratory	20 μm	8 nm	0.63 MHz
74	Ciliated Epithelial Cell (Trachea)	Respiratory	15 μm	8 nm	0.84 MHz
75	Goblet Cell	Digestive / Respiratory	15 μm	8 nm	0.84 MHz
76	Club Cells (Bronchiolar)	Lung	10 μm	8 nm	1.26 MHz
77	Type I pneumocyte	Lung	30 μm	8 nm	420 kHz
78	Type II pneumocyte	Lung	15 μm	8 nm	0.84 MHz
79	Podocito	Kidney	20 μm	8 nm	0.63 MHz
80	Mesangial Cell	Kidney	12 μm	8 nm	1.05 MHz
81	Proximal Tubule Cell	Kidney	20 μm	8 nm	0.63 MHz
82	Distal Tubule Cell	Kidney	15 μm	8 nm	0.84 MHz
83	Principal Cell (Collecting Tubule)	Kidney	12 μm	8 nm	1.05 MHz
84	Urothelium (Umbrella Cell)	Bladder	25 μm	8 nm	0.50 MHz
85	Enterocyte	Small intestine	20 μm	8 nm	0.63 MHz
86	Paneth cell	Small intestine	12 μm	8 nm	1.05 MHz
87	M-cell (Microfold)	Intestine (Peyer's patches)	15 μm	8 nm	0.84 MHz

88	Colonocito	Colon	20 μm	8 nm	0.63 MHz
89	Hepatocito	Liver	25 μm	8 nm	0.50 MHz
90	Cholangiocyte	Biliary ducts	10 μm	8 nm	1.26 MHz
91	Pancreatic Acinar Cell	Pancreas (Exocrine Gland)	25 μm	8 nm	0.50 MHz
92	Centroacinar Cell	Pancreas (Exocrine Gland)	8 μm	8 nm	1.58 MHz
93	Salivary Acinar Cell	Salivary Gland	20 μm	8 nm	0.63 MHz
94	Parietal (Gastric) Cell	Stomach	20 μm	8 nm	0.63 MHz
95	Chief Cell (Gastric)	Stomach	15 μm	8 nm	0.84 MHz
96	G cell (Gastric)	Stomach	12 μm	8 nm	1.05 MHz
97	Pigment Epithelium Cell	Rain (Retina)	14 μm	8 nm	0.90 MHz
98	Corneal Epithelial Cells	Ocular (Cornea)	20 μm	8 nm	0.63 MHz
99	Lens Fiber	Eye (Translucent)	8 μm	8 nm	1.58 MHz
100	Pericito	Capillaries	10 μm	8 nm	1.26 MHz

CELLS OF THE ENDOCRINE SYSTEM

101	Chromaffin cell	Adrenal gland	20 μm	8 nm	0.63 MHz
102	Glomerular Zone Cell	Adrenal gland	15 μm	8 nm	0.84 MHz
103	Zona Fasciculata Cell	Adrenal gland	18 μm	8 nm	0.70 MHz
104	Reticular Zone Cell	Adrenal gland	12 μm	8 nm	1.05 MHz
105	Thyroid Follicular Cell	Thyroid	15 μm	8 nm	0.84 MHz
106	Parafollicular Cell (C Cell)	Thyroid	12 μm	8 nm	1.05 MHz
107	Parathyroid Principal Cell	Parathyroid	8 μm	8 nm	1.58 MHz
108	Parathyroid Oxyphil Cell	Parathyroid	14 μm	8 nm	0.90 MHz
109	Pancreatic Alpha Cell	Pancreas (Endocrine System)	15 μm	8 nm	0.84 MHz
110	Pancreatic Beta Cell	Pancreas (Endocrine System)	14 μm	8 nm	0.90 MHz
111	Pancreatic Delta Cell	Pancreas (Endocrine System)	12 μm	8 nm	1.05 MHz
112	Pancreatic Polypeptide Cell	Pancreas (Endocrine System)	12 μm	8 nm	1.05 MHz
113	Somatotrope	Anterior Pituitary Gland	15 μm	8 nm	0.84 MHz
114	Lactotrope	Anterior Pituitary Gland	15 μm	8 nm	0.84 MHz
115	Corticotrope	Anterior Pituitary Gland	12 μm	8 nm	1.05 MHz
116	Thyrotrope	Anterior Pituitary Gland	12 μm	8 nm	1.05 MHz
117	Gonadotropin	Anterior Pituitary Gland	12 μm	8 nm	1.05 MHz
118	Pituicito	Posterior Pituitary Gland	10 μm	8 nm	1.26 MHz
119	Pinealocito	Pineal gland	15 μm	8 nm	0.84 MHz
120	Enteroendocrine Cell	Gastrointestinal System	10 μm	8 nm	1.26 MHz

CELLS OF THE REPRODUCTIVE SYSTEM

121	Oocyte	Ovary	120 μm	8 nm	105 kHz
122	Granulosa Cell	Ovary	7 μm	8 nm	1.80 MHz
123	Theca cell	Ovary	15 μm	8 nm	0.84 MHz
124	Luteal Cell	Ovary (Corpus Luteum)	30 μm	8 nm	420 kHz
125	Uterine Epithelial Cell	Uterus (Endometrium)	15 μm	8 nm	0.84 MHz
126	Uterine Stromal Cells	Uterus (Endometrium)	12 μm	8 nm	1.05 MHz
127	Myometrial Cell	Uterus	8 μm	8 nm	1.58 MHz
128	Cervical Epithelial Cells	Cervix	20 μm	8 nm	0.63 MHz
129	Vaginal Epithelial Cell	Vagina	30 μm	8 nm	420 kHz
130	Syncytiotrophoblast (section)	Placenta	40 μm	8 nm	315 kHz
131	Cytotrophoblast	Placenta	15 μm	8 nm	0.84 MHz
132	Leydig cell	Testicle	18 μm	8 nm	0.70 MHz
133	Sertoli cell	Testicle	30 μm	8 nm	420 kHz
134	Spermatogonium	Testicle	12 μm	8 nm	1.05 MHz
135	Primary spermatocyte	Testicle	18 μm	8 nm	0.70 MHz
136	Secondary spermatocyte	Testicle	12 μm	8 nm	1.05 MHz
137	Spermatid	Testicle	8 μm	8 nm	1.58 MHz
138	Spermatozoon (head)	Testicle	4 μm	8 nm	3.15 MHz
139	Prostatic Epithelial Cell	Prostate	15 μm	8 nm	0.84 MHz
140	Myoepithelial Cell	Glands	10 μm	8 nm	1.26 MHz

STEM AND PROGENITOR CELLS

141	Embryonic Stem Cells	Embryo	12 μm	8 nm	1.05 MHz
142	Hematopoietic Stem Cell	Bone Marrow	10 μm	8 nm	1.26 MHz
143	Mesenchymal Stem Cells	Connective Tissue	20 μm	8 nm	0.63 MHz
144	Neural Stem Cell	Nervous system	10 μm	8 nm	1.26 MHz
145	Epidermal Stem Cell	Fur	8 μm	8 nm	1.58 MHz
146	Intestinal Stem Cell	Intestine	8 μm	8 nm	1.58 MHz
147	Myeloid Progenitor Cell	Bone Marrow	14 μm	8 nm	0.90 MHz
148	Lymphoid Progenitor Cell	Bone Marrow	10 μm	8 nm	1.26 MHz
149	Proerythroblast	Bone Marrow	15 μm	8 nm	0.84 MHz
150	Myeloblast	Bone Marrow	14 μm	8 nm	0.90 MHz

ADDITIONAL CELLS

151	Lymphoblast	Bone Marrow	12 μm	8 nm	1.05 MHz
152	Monoblast	Bone Marrow	15 μm	8 nm	0.84 MHz
153	Angioblast	Endothelial Progenitor	12 μm	8 nm	1.05 MHz
154	Hair Follicle Stem Cells	Fur	8 μm	8 nm	1.58 MHz
155	Hepatoblasto	Fetal Hepatic Tissue	15 μm	8 nm	0.84 MHz
156	Nephroblast	Fetal Renal System	10 μm	8 nm	1.26 MHz
157	Cardiac Stem Cells	Heart	10 μm	8 nm	1.26 MHz
158	Trophoblastic Cell	Embryo	18 μm	8 nm	0.70 MHz
159	Epiblast cell	Embryo	10 μm	8 nm	1.26 MHz
160	Hypoblast cell	Embryo	8 μm	8 nm	1.58 MHz
161	Primitive Node Cell	Embryo	12 μm	8 nm	1.05 MHz
162	Neural Crest Cell	Embryo	10 μm	8 nm	1.26 MHz
163	Primordial Germ Cell	Fetal Gonads	15 μm	8 nm	0.84 MHz
164	Ameloblast	Served	20 μm	8 nm	0.63 MHz
165	Odontoblast	Served	18 μm	8 nm	0.70 MHz
166	Cementoblasto	Served	15 μm	8 nm	0.84 MHz
167	Peritubular Myoid Cell	Testicle	8 μm	8 nm	1.58 MHz
168	Bowman's Capsule Cell	Kidney	15 μm	8 nm	0.84 MHz
169	Interstitial Cells of Cajal	Gastrointestinal Tract	10 μm	8 nm	1.26 MHz
170	Hepatic Stellate Cell (Ito)	Liver	12 μm	8 nm	1.05 MHz
171	Pancreatic Stellate Cell	Pancreas	10 μm	8 nm	1.26 MHz
172	Folliculostellate cell	Anterior Pituitary Gland	10 μm	8 nm	1.26 MHz
173	Interstitial Cells of the Kidney	Kidney	12 μm	8 nm	1.05 MHz
174	Macula Densa Cell	Kidney	10 μm	8 nm	1.26 MHz
175	Juxtaglomerular cells	Kidney	15 μm	8 nm	0.84 MHz

176	Clear Cell (Cell Club)	Lung	10 μm	8 nm	1.26 MHz
177	Brush Cell	Respiratory System/Gastrointestinal Tract	12 μm	8 nm	1.05 MHz
178	Hering cell	Liver	8 μm	8 nm	1.58 MHz
179	Radial Glial Cell	CNS during development	10 μm	8 nm	1.26 MHz
180	Müller Glial Cell	Rain (Retina)	10 μm	8 nm	1.26 MHz
181	Bergmann glial cell	Cerebellum	8 μm	8 nm	1.58 MHz
182	Spider Cell (Cardiac)	Heart	15 μm	8 nm	0.84 MHz
183	His bundle cell	Heart	20 μm	8 nm	0.63 MHz
184	Purkinje fibers	Heart	30 μm	8 nm	420 kHz
185	Sinoatrial Node Cell	Heart	8 μm	8 nm	1.58 MHz
186	AV Node Cell	Heart	10 μm	8 nm	1.26 MHz
187	Thymic Epithelial Cell	Timo	15 μm	8 nm	0.84 MHz
188	Military Cell	Timo	10 μm	8 nm	1.26 MHz
189	Follicular Dendritic Cell	Lymphatic node	12 μm	8 nm	1.05 MHz
190	Fibroblastic Reticular Cell	Lymphoid Tissue	15 μm	8 nm	0.84 MHz
191	Bone Marrow Stromal Cells	Bone Marrow	20 μm	8 nm	0.63 MHz
192	Synoviocyte	Joints	15 μm	8 nm	0.84 MHz
193	Decidual Cell	Endometrial tissue (gestation)	25 μm	8 nm	0.50 MHz
194	Hofbauer cell	Placenta	18 μm	8 nm	0.70 MHz
195	Intercalated Cell (Renal)	Kidney	12 μm	8 nm	1.05 MHz
196	Small granule cell (Lung)	Lung	10 μm	8 nm	1.26 MHz
197	Olfactory Support Cell	Olfactory epithelium	12 μm	8 nm	1.05 MHz
198	Basal (Olfactory) Cell	Olfactory epithelium	8 μm	8 nm	1.58 MHz
199	Deiters cell	Inner Ear	10 μm	8 nm	1.26 MHz
200	Tympanic Cavity	Bone Marrow	12 μm	8 nm	1.05 MHz